**ORIGINAL ARTICLE**

# Influence of a power plant in Ezhou City on the groundwater environment in the nearby area

Chu Wu[1] · Xiong Wu[1] · Ge Zhu[1] · Cheng Qian[1] · Wen-Ping Mu[2] · Yu-zhe Zhang[1]

## Abstract

To effectively protect shallow groundwater and to evaluate the environmental impact of groundwater, we set up a monitoring network of 30 monitoring wells and collected 11 water samples from the wells during the rainy and dry seasons. Hydrochemical characteristics of the shallow groundwater were identified with the Piper and Gibbs diagrams. Groundwater quality was assessed with the single standard index method and the entropy-weighted water quality index. Finally, we used a numerical simulation of the impact of the power plant operation on the groundwater environment. The average abundance of the major ions in groundwater from the dry to the wet season occurred in the following orders: $Ca^{2+} > Na^+ > Mg^{2+} > K^+$ for cations and $HCO_3^- > SO_4^{2-} > Cl^-$ for anions. The shallow groundwater usually has elevated hardness and alkalinity values comparison with the standard values. The dominant hydrochemical facies of the groundwater is the $HCO_3$–Ca type. Rock weathering is likely to be the dominant process that controls the groundwater chemical composition. Groundwater in the study area is suitable for drinking under ordinary conditions, according to the single standard index method and the entropy-weighted water quality index. However, the groundwater quality has been influenced by anthropogenic activities (including near the west Ash Yard and Huangji Sunaba). Numerical modeling shows that leakage during abnormal operating conditions is of limited extent within the boundary of the simulated area and does not enter into the Yangtze River. Overall, it is necessary to carry out effective anti-seepage and pollution control measures to ensure that shallow groundwater is not contaminated.

**Keywords** Hydrogeochemistry · Entropy weighted · Groundwater quality · Numerical simulation · Contaminant transport

## Introduction

Water resources in China are unevenly distributed over space and time (Yan and Chen 2013), and groundwater is considered to be a dependable source of uncontaminated water (Chanchal et al. 2015). As a water resource for sustainable development, groundwater use is an essential, complex, and permanent issue because when surface water shortages occur, the original environmental and aquatic ecological equilibriums are strongly affected (Gohari et al. 2013). The sustainable management of water resources usually requires a balance to be achieved between the amount of water that is used for social and economic needs against the amount that

is required to maintain environmental values (Venkataraman et al. 2016). However, with the rapid development of the economy and society, groundwater in many areas across the world is in short supply and has been affected or polluted by human activities (Qian et al. 2016; Li et al. 2014). It is very important to protect groundwater resources, and governments and businesses can play an important role in protecting and improving water quality through raising public awareness and recycling water (Li et al. 2018).

Groundwater pollution, one of the most serious and widespread issues in China, refers to the phenomenon of the progressive deterioration of water quality under the influence of human activities (Li et al. 2016b). Furthermore, the results of water quality evaluations often include effects from natural factors that may bias the evaluation results and are not necessarily useful in defining effective measures for groundwater pollution prevention (Peng et al. 2017; Vandenbohede et al. 2011). Qian et al. (2016) used single-parameter comparisons and fuzzy comprehensive evaluations to analyze the degree of human influence on groundwater quality in the

✉ Xiong Wu
wuxiong@cugb.edu.cn

1 School of Water Resource and Environment, China University of Geosciences, Beijing 100083, China

2 College of Geoscience and Surveying Engineering, China University of Mining and Technology, Beijing 100083, China

Ordos Basin, central China. In addition, fuzzy c-means clustering and principal components analysis were used to evaluate the impact of human activities on groundwater chemistry in the coastal plain of Turkey (Güler et al. 2012). Although each method has advantages for assessing the influence of human activities on groundwater quality, the entropy-based weighted technique can avoid having too many factors that need to be considered and can clearly delineate water quality categories and express whether the variables involved in the evaluation meet the decision-making criteria of functional areas (Islam et al. 2017; Varnosfaderany et al. 2009).

The power plants that are the subject of this study are located in Ezhou City in southern China, along the Yangtze River, where a large quantity of clean water is needed for the agriculture, fisheries, and poultry industries. Although there are enough available water sources at present, surface water pollution is becoming more and more aggravated, and groundwater pollution has also become serious. These factors are likely to adversely affect the balance of the water resource supply and the regional water demands (He and Xu 2010). It has been shown that the regional groundwater is in serious danger of being contaminated due to leakage of some organic pollutants, caused by abnormal operating conditions, which will eventually enter the groundwater supply (Wu et al. 2017). To improve the groundwater quality and protect the water sources of the Yangtze River, a systematically managed framework must be used (Hayat and Baba 2017).

To protect shallow groundwater and evaluate the environmental impacts on groundwater, it is necessary to first understand its hydrochemical characteristics and the factors that influence groundwater quality (Qian et al. 2016; Xiao et al. 2014). Due to the emphasis on groundwater quality, the number of real-time monitoring wells has been installed in the area. When sudden groundwater pollution occurs from leakage during abnormal operating conditions, shallow groundwater quality indexes are obtained from adjacent monitoring wells, and these real-time data can be used to improve simulation accuracy (Shao et al. 2016). The entropy-weighted water quality index (EWQI) can correctly calculate the groundwater quality, which can be ranked on the basis of the groundwater quality standards (Amiri et al. 2014; Islam et al. 2017).

In addition, numerical simulation models have become a powerful tool to describe and study physical systems and related phenomena. They are applied in this field of science and engineering to describe hydrologic phenomena, groundwater flow fields, and the movement of contaminants, and to evaluate or predict the groundwater environmental impacts of contaminant migration (Karatzas 2017). Many researchers have used numerical methods to forecast groundwater flow based on conceptual hydrogeological models, which have been further developed as computers continue to facilitate

the construction of complex models (Lap et al. 2007; Shao et al. 2016). For describing the evolution of the contaminant scope as essential in environmental impact assessments, the longitudinal distributed mean concentration and the excessive scope from long-timescale evolution are used to determine some characteristic parameters, including the duration and the critical length of the contaminant scope (Wu et al. 2015; Zeng et al. 2014).

However, a thorough understanding of hydrochemical characteristics and environmental risks, as well as the factors influencing groundwater quality, is vital for decision making in any particular region. In this study, we carried out a groundwater sampling program that analyzed the hydrochemical parameters to determine the hydrochemical characteristics of groundwater and the factors controlling its chemical composition. The characterization of groundwater quality ranks was performed by comparing the entropy-weighted water quality index to the single standard index method. Finally, a numerical model of GMS software was set up to simulate and predict the migration of potential pollutants during leakage under abnormal operating conditions in shallow groundwater, which helps in the environmental risk assessment of these areas. Considering all of these factors, therefore, this study was designed to outline the hydrochemical characteristics and processes, to calculate drinking water quality ranks, and to perform an environmental risk assessment for the power plant of Ezhou City using the aforementioned approaches for scientific justification and decision making.

## Study area

The study area (power plant of Ezhou) is located in the Huarong district of Ezhou City, which is in the eastern part of the Hubei Province and is on the south bank of the middle Yangtze River (Fig. 1). Topographically, the terrain flats, with an overall trend of topographic highs to lows from southeast to northwest, belong to the second terraces of the Yangtze River. There are four distinct seasons with ample sunshine and rainfall. Precipitation occurs throughout the year, particularly, during the summer. The annual average precipitation is 1338.9 mm, and evapotranspiration is 1455.98 mm, which occurs primarily from April to September. The study area is in the subtropical monsoon climate zone, and the annual average relative humidity is 76%. The annual average temperature of this area is 17.2 °C, and the extreme maximum and minimum temperatures are 40.7 and $-12.4$ °C, respectively.

The region is underlain by a range of sediments. The shallowest sedimentary unit of Quaternary age is approximately 45 m thick. These sediments overlie Devonian quartzose sandstone and the Cretaceous argillaceous sandstone, which
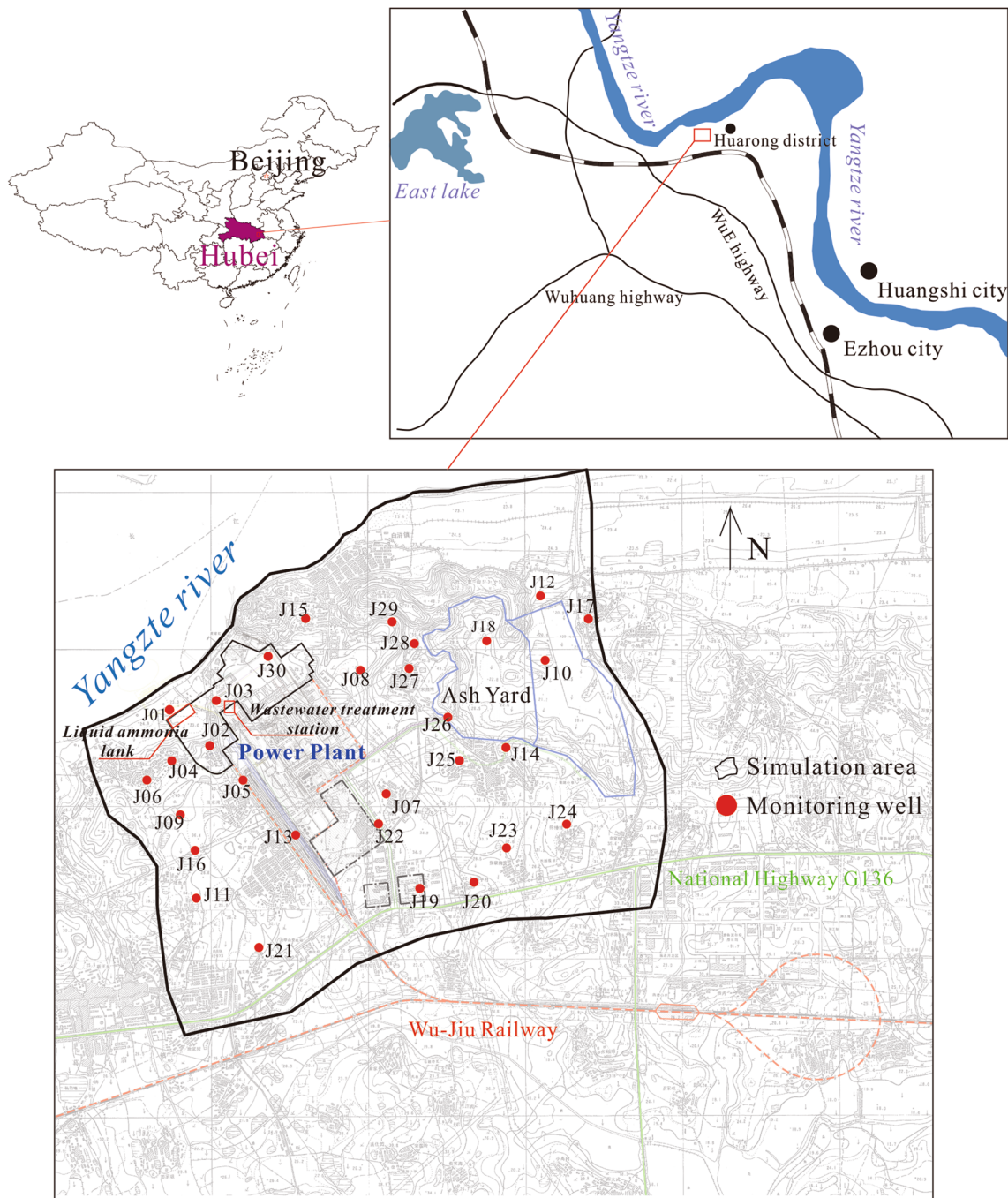
**Fig. 1** Location of the study area and monitoring well locations

was influenced by the subsiding belts of the Neocathaysian system.

The immediate base of the phreatic aquifer mainly consists of silty clay and clay as the relative aquiclude, with a permeability coefficient of 6.4e-5–1.7e-3 m/d. The phreatic water has a weak connection with the underlying fissure water, which is composed of eluvial silty clay with crushed stone and underlying bedrock. The groundwater level is shallow with depths of 0.4–3.6 m. Shallow groundwater is mainly recharges by the infiltration of atmospheric rainfall, which follows the terrain surface slope from the south to the north of the low water level, and ultimately drains into the Yangtze River.

## Materials and methods

### Sample collection and analysis

In this study area, groundwater from the phreatic aquifer was sampled during the dry season (March 2013) and the wet season (October 2013), and 11 groundwater samples were collected in the power plant. The monitoring wells were evenly distributed in the study area (Kim 2015), as shown in Fig. 1. Sample collection, handling, and storage follow the standard procedures that are recommended by the Chinese Ministry of Water Resources (Qian et al. 2016). We sent these samples to the Pony Testing International Group for the measurement of 25 parameters, including major cations ($K^+$, $Na^+$, $Ca^{2+}$, $Mg^{2+}$), major anions ($HCO_3^-$, $SO_4^{2-}$, $Cl^-$), fluoride ($F^-$), three nitrogen species ($NO_3^-$-N, $NO_2^-$–N, $NH_4^+$–N), heavy metals, and total hardness (TH). Among these parameters, $Na^+$ and $K^+$ were determined using a flame photometer; $SO_4^{2-}$, $Cl^-$, and $HCO_3^-$ were analyzed using ion chromatography; $Ca^{2+}$, $Mg^{2+}$, $F^-$, three nitrogen, heavy metals, and Fe were determined by spectrophotometry; and pH, electric conductivity (EC), total dissolved solids (TDS), and others were analyzed immediately with a portable instrument from HANNA (HI9828). The accuracy of the water quality tests was controlled using blank samples, parallel samples, and internal standards, and the percentage of charge balance error (%CBE) was calculated to be less than 5%, suggesting that the accuracy of each index meets the quality requirements.

### Methods

The shallow groundwater quality can be assessed by the single standard index method, which can intuitively reflect the parameters and groundwater quality. The single standard index method for determining the evaluation criteria consists of a constant value and an interval value (as pH) of groundwater quality, as shown in Eqs. 1 and 2, respectively (Zhang et al. 2011):

$$P_i = \frac{C_i}{C_{si}}, \tag{1}$$

where $P_i$ is the standard index of the parameter $i$; $C_i$ is the monitoring concentration of the parameter $i$ (mg/L); and $C_{si}$ is the standard concentration of the parameter $i$ (mg/L).

$$\begin{cases} P_{pH} = \dfrac{7.0 - pH}{7.0 - pH_{min}}, & pH \le 7 \\ P_{pH} = \dfrac{pH - 7.0}{pH_{max} - 7.0}, & pH > 7, \end{cases} \tag{2}$$

where $P_{pH}$ is the standard index of pH; pH is the monitoring value; $pH_{max}$ is the upper limit of pH in the standard; and $pH_{min}$ is the lower limit of pH in standard.

The EWQI is applied to characterize groundwater quality due to its features that can make full use of all available parameters to evaluate groundwater quality and give comprehensive groundwater-quality information (Islam et al. 2017; Li et al. 2010; Su et al. 2017). The three steps that are used to calculate the EWQI are given below (Li et al. 2010).

Supposing that there are $m$ groundwater samples and that each sample has $n$ hydrochemical parameters, the first step is the calculation of the eigenvalue matrix, $X$, which is associated with all the samples in the following equation:

$$X = \begin{bmatrix} x_{11} & x_{12} & \cdots & x_{1n} \\ x_{21} & x_{22} & \cdots & x_{2n} \\ \vdots & \vdots & \ddots & \vdots \\ x_{m1} & x_{m2} & \cdots & x_{mn} \end{bmatrix}. \tag{3}$$

Then, using Eq. 4, the eigenvalue matrix $X$ is converted into a standard-grade matrix $Y$ in Eq. 5:

$$y_{ij} = \frac{x_{ij} - (x_{ij})_{min}}{(x_{ij})_{max} - (x_{ij})_{min}} \tag{4}$$

$$Y = \begin{bmatrix} y_{11} & y_{12} & \cdots & y_{1n} \\ y_{21} & y_{22} & \cdots & y_{2n} \\ \vdots & \vdots & \ddots & \vdots \\ y_{m1} & y_{m2} & \cdots & y_{mn} \end{bmatrix}. \tag{5}$$

The ratio of parameter index value $j$ and the $i$ sample and the entropy $e_j$ of the $j$ parameter are calculated with Eqs. 6 and 7, respectively:

$$P_{ij} = \frac{y_{ij}}{\sum_{i=1}^{m} y_{ij}} \tag{6}$$

$$e_j = -\frac{1}{\ln m} \sum_{i=1}^{m} P_{ij} \ln P_{ij}. \tag{7}$$

The smaller the amount of entropy, the bigger the effectiveness of the $j$ parameter. Then, calculate the weight $w_j$ of the $j$ parameter using the following equation:

$$w_j = \frac{1 - e_j}{\sum_{j=1}^{n} (1 - e_j)}. \tag{8}$$

The second step is the determination of the quantitative rating scale $q_j$ of the $j$ parameter using the following equation:

$$\begin{cases} q_j = \dfrac{C_j}{S_j} \times 100 \\ q_{pH} = \dfrac{C_{pH} - 7}{8.5 - 7} \times 100 \end{cases}, \qquad (9)$$

where $C_j$ is the concentration of the $j$ parameter (mg/L), $C_{pH}$ is the value of pH, and $S_j$ is the permissible limit of the standard for drinking water quality of China of $j$ parameter (mg/L).

The EWQI is calculated using Eq. 10 in the third step:

$$\mathrm{EWQI} = \sum\nolimits_{j=1}^{n} w_j q_j. \qquad (10)$$

Based on the entropy-weighted water quality index, groundwater quality can be categorized into five ranks for drinking purposes in the study area (Kamrani et al. 2016), as shown in Table 1.

Numerous methods have been applied to evaluate groundwater quality, and each has its own characteristics and can be used in different applications. The entropy-based weighted theory can estimate the weights of groundwater hydrochemical parameters that ignore the artificial weight dividing, and it can also clearly delineate water quality categories and properly assess water pollutant ranks (Islam et al. 2017). Comparing the entropy-weighted water quality index and the single standard index methods is an appropriate approach for scientific justification and sound decision making. Therefore, this study presents reasonable results of a groundwater quality assessment. In addition, numerical modeling was conducted using the 3D finite-difference groundwater flow model-GMS (Karatzas 2017). Then, some other models were linked to the GMS model, including MT3D, which is a modular three-dimensional transport model. MT3D simulates advection in complex steady-state and transient flow fields, anisotropic dispersion, and multispecies reactions, and it can simulate or assess natural attenuation within a contaminant plume. Numerical models based on the advection–diffusion equation and the continuity equation have been widely used to forecast groundwater environmental impacts in previous studies (Lap et al. 2007; Shao et al. 2016).

# Results and discussion

## Chemical characteristics of groundwater

### Hydrochemical parameters statistics

Here, we provide a statistical summary of the hydrochemical parameters of shallow groundwater in the dry and wet seasons. The heavy metals that did not exceed the detection value (GB/T14848-93 in China) (Bureau of Quality and Technical Supervison of China (1994)), including Zn, Al,

**Table 1** Classification of the entropy-weighted water quality index (EWQI)

| EWQI | < 25 | 25–50 | 50–100 | 100–150 | > 150 |
|---|---|---|---|---|---|
| Rank | I | II | III | IV | V |
| Water quality | Excellent | Good | Medium | Poor | Extremely poor |

**Table 2** Statistical summary of chemical parameters

| Parameters | Groundwater from dry season | | | Groundwater from wet season | | |
|---|---|---|---|---|---|---|
| | Min | Max | Mean | Min | Max | Mean |
| $K^+$ | 0.73 | 27.1 | 4.48 | 0.84 | 27.1 | 4.83 |
| $Na^+$ | 13.9 | 56.1 | 30.65 | 15.5 | 62.8 | 31.90 |
| $Ca^{2+}$ | 57.3 | 598 | 134.07 | 42.4 | 231 | 107.13 |
| $Mg^{2+}$ | 12.1 | 56.6 | 27.55 | 12 | 43.1 | 22.75 |
| $Cl^-$ | 13.4 | 177 | 65.35 | 17.6 | 81 | 46.52 |
| $SO_4^{2-}$ | 19 | 1320 | 215.17 | 29.8 | 436 | 140.54 |
| $HCO_3^-$ | 160 | 378 | 293.55 | 123 | 398 | 247.18 |
| $NO_3^-$–N | < 0.04 | 15.3 | 4.85 | < 0.04 | 12.6 | 4.34 |
| $NO_2^-$–N | < 0.001 | 0.74 | 0.28 | < 0.001 | 0.02 | 0.01 |
| $NH_3$–N | < 0.02 | 0.41 | 0.17 | < 0.02 | 0.44 | 0.15 |
| $F^-$ | 0.14 | 1.54 | 0.47 | 0.17 | 1.52 | 0.50 |
| TH | 55 | 1790 | 413.18 | 198 | 764 | 365.91 |
| TDS | 269 | 2384 | 641.82 | 304 | 1100 | 537.55 |
| pH | 7.24 | 7.92 | 7.57 | 7.06 | 7.32 | 7.22 |

Units: mg/L, except pH; <, below the limit of detection

Se, and Cu, are not described in detail here. As shown in Table 2, although $K^+$ is one of the essential elements for human health, it is widely thought that the concentration of $K^+$ is generally low in groundwater. The mean concentrations of $K^+$ are 4.48 and 4.83 mg/L, and they did not change significantly from the dry to the wet season. Groundwater, with a mean $Cl^-$ concentration of 65.35 and 46.52 mg/L, exceeds the mean concentration of $Na^+$ (30.65 and 31.90 mg/L) in the dry and wet seasons, respectively, which may be due to cation exchange (Li et al. 2013; Islam et al. 2017). $Ca^{2+}$ and $Mg^{2+}$ in groundwater mainly come from the dissolution of carbonate minerals and cation exchange. The mean $Ca^{2+}$ concentrations of 134.07 and 107.13 mg/L are higher than that of $Mg^{2+}$ (27.55 and 22.75 mg/L), during the dry and wet seasons, respectively, also indicating that the dissolution of calcite may be a dominant factor governing the groundwater chemistry (Garcia et al. 2001; Qian et al. 2016). Furthermore, the highest concentration of $Ca^{2+}$ (J18) in the dry season is 598.00 mg/L, which exceeds the permissible limit (400 mg/L). The national standards set the concentration limit of $SO_4^{2-}$ at 250 mg/L, and the concentration of $SO_4^{2-}$ is likely to occur from the dissolution of sulfate-bearing minerals and the oxidation of sulfides (Islam et al. 2017). In the study sites, the mean concentrations of $SO_4^{2-}$ are 215.70 and 140.54 mg/L in dry and wet seasons, respectively. However, two samples exceed the permissible limit. As one of the major anions, the concentration of $HCO_3^-$ primarily occurs due to carbonate dissolution, with average concentrations of 293.55 and 247.18 mg/L in the dry and wet seasons, respectively, and with no values that exceed the permissible limit (500 mg/L). Based on the above analysis, the major cations and anions of the hydrochemical parameters have remained relatively unchanged in the dry and wet seasons, but the two samples from monitoring wells J01 and J18 are exceptions because of their special location. According to the average concentration, the abundance of the major ions for groundwater in the dry and wet seasons is as follows: $Ca^{2+} > Na^+ > Mg^{2+} > K^+$ for cations and $HCO_3^- > SO_4^{2-} > Cl^-$ for anions.

Groundwater nitrogen and fluoride pollution is a common concern globally. In general, three nitrogen compounds, $NO_3^-$–N, $NO_2^-$–N, and $NH_3$–N, suggest groundwater contamination due to the use of chemical fertilizer, industrial production, and feces. They can be used for estimating the pollution of groundwater, and they have transformational relationships under different conditions (Su et al. 2017; Winton et al. 2016). The concentration of $NO_3^-$–N in the dry and wet seasons varies from < 0.04 to 15.30 mg/L and < 0.04–12.60 mg/L (< below the limit of detection), while $NO_2^-$N ranges from < 0.001 to 0.74 mg/L and < 0.001–0.02 mg/L, and $NH_3$–N ranges from < 0.02 to 0.41 mg/L and < 0.02–0.44 mg/L, during the dry and wet seasons, respectively. The mean
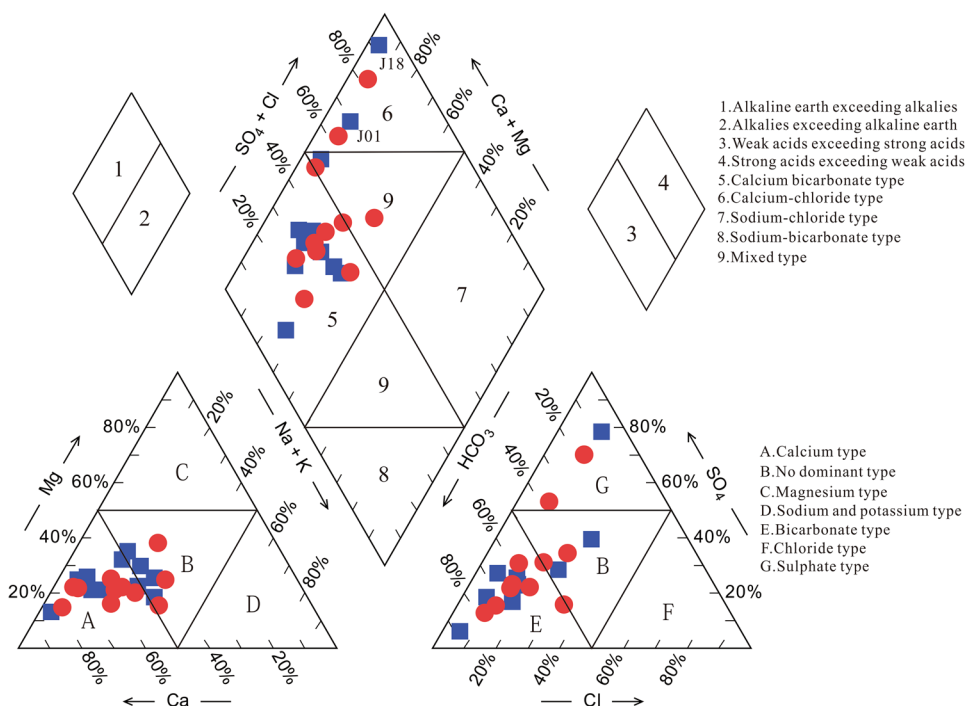
concentration of the three nitrogen compounds are as follows: $NO_3^-$–N > $NO_2^-$–N > $NH_3$–N. The high concentrations of $NO_3^-$–N and low concentrations of $NO_2^-$–N and $NH_3$–N in groundwater indicate that the groundwater has been polluted in the past and that either the pollution source has been removed or that nitrogen is being removed by biochemical reactions in the aquifer (Zhang et al. 2015). As essential trace elements in the human body, and the average concentrations of $F^-$ in these wells are 0.47 and 0.50 mg/L in the dry and wet seasons, respectively, which are under the limit value in the national standard (1 mg/L in drinking water), except the $F^-$ maximum concentration of 1.54 and 1.52 mg/L in the monitoring well (J18) near the west Ash Yard.

TDS is a significant parameter used to determine the quality of groundwater. All of the water samples in the dry and wet seasons are classified as freshwater type in the study area because their respective TDS mean concentrations of 641.82 and 537.55 mg/L are less than 1000 mg/L. The TDS concentrations of 2384 mg/L (J18) in the dry season and 1100 mg/L (J01) in the wet season are located at the west Ash Yard and the Huangji Sunaba, respectively, and the Huangji Sunaba is near the bank of the Yangtze River. The mean TH concentrations are 641.82 and 365.91 mg/L in the dry and wet seasons, respectively. Because the maximum concentration of TH is 1790.00 mg/L, the mean concentration exceeds the permissible limit of 450 mg/L in the dry season. In addition, two samples slightly exceed the permissible limit in the groundwater drainage area (J01) and near the west Ash Yard (J12) of the study area. The Chinese standards for drinking water quality require that the pH ranges from 6.5 to 8.5; in this study area, the mean values of pH are 7.57 and 7.22, respectively, indicating that the shallow groundwater is slightly alkaline in the study area. Overall, the results of the hydrochemical analysis have shown that the chemical composition of the groundwater in the dry and wet seasons have not clearly fluctuated, except for the samples from the monitoring well near the west Ash Yard and Huangji Sunaba and that the shallow groundwater has a slightly high hardness and alkalinity. Human activities and the natural geological environment are important influences on the chemical composition of shallow groundwater in the study area.

## Hydrochemical facies

Piper trilinear diagrams have been widely used to understand the hydrogeochemical regime of a study area (Ahada and Suthar 2017; Li et al. 2013; Qian et al. 2016). As shown in Fig. 2, most of the samples from the dry and wet seasons fall in zone 5, which suggests that the carbonate

**Fig. 2** Piper diagram of shallow groundwater (after Qian et al. 2016; blue squares for dry season data and red circles for wet season data)



1.Alkaline earth exceeding alkalies
2.Alkalies exceeding alkaline earth
3.Weak acids exceeding strong acids
4.Strong acids exceeding weak acids
5.Calcium bicarbonate type
6.Calcium-chloride type
7.Sodium-chloride type
8.Sodium-bicarbonate type
9.Mixed type

A.Calcium type
B.No dominant type
C.Magnesium type
D.Sodium and potassium type
E.Bicarbonate type
F.Chloride type
G.Sulphate type

hardness exceeds 50% and that weak acids exceed strong acids, except for the two special samples (J01 and J18), which have high concentrations of $Ca^{2+}$ and $SO_4^{2-}$, as described in the hydrochemical parameters section. With respect to the anions, most of the shallow groundwater samples plot in zone E, suggesting the dominance of $HCO_3$, and the cations plot in zone A and B, which also indicates the dominance of Ca. The dominant hydrochemical facies of the shallow groundwater is the $HCO_3$–Ca type.

## Factors influencing the chemical composition of groundwater

The formation of groundwater chemistry is usually influenced by three factors, including rock weathering, evaporation, and crystallization and precipitation. The dominant factor is often determined by Gibbs diagrams (Li et al. 2013; Murkute 2014). However, the extent and degree of human activity is difficult to quantify, so the results do not necessarily mean that groundwater formation mechanisms are

**Fig. 3** Gibbs plots that illustrate the mechanisms governing shallow groundwater chemistry (after Gibbs 1970)
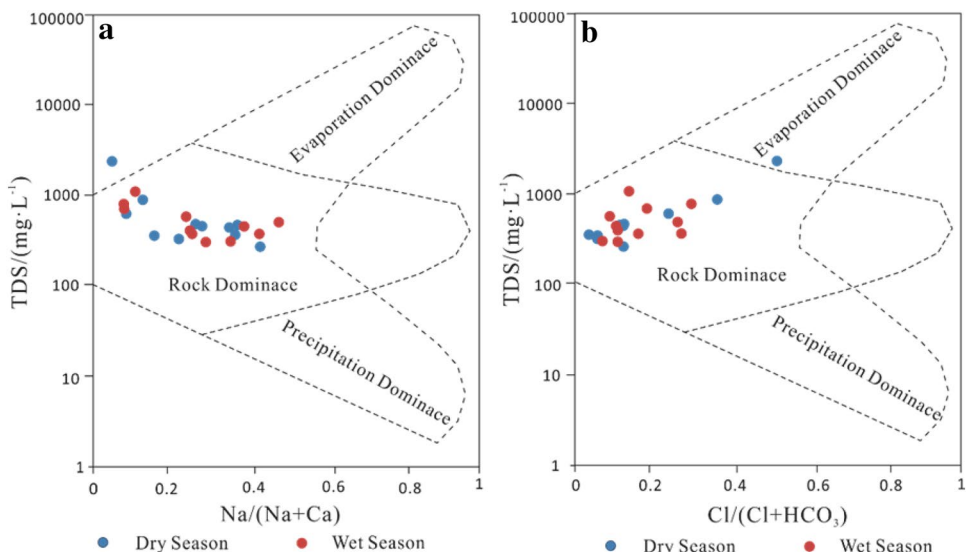
completely free from human interference (Li et al. 2016a). Most of the samples in this study fall within the rock-dominated zone of Gibbs diagrams (Fig. 3), suggesting that the major ion chemistry of the shallow groundwater in the dry and wet seasons was essentially controlled by rock weathering (Marghada et al. 2012; Murkute 2014). There is a shallow groundwater sample that has Na/(Na + Ca) ratios < 0.2 and a relatively high TDS value of 2384 mg/L in the dry season near the west Ash Yard (Fig. 3a). Similarly, Fig. 3b shows that a sample from the dry season near the west Ash Yard belongs to the evaporation dominance zone, with Cl/(Cl + HCO$_3$) ratios > 0.5. This peculiar sample does not affect the finding that the overall shallow groundwater chemistry formation mechanisms were controlled by rock weathering.

## Groundwater quality assessment

The permissible limits of the Quality Standard for Groundwater (class III) (QSGW) were employed to assess the suitability of these samples for drinking purposes. The results show that the major parameters of concern are TH, pH, TDS, NO$_2^-$–N, F$^-$, and SO$_4^{2-}$ (Table 3).

The evaluation results of assessing groundwater quality using the single standard index method with the QSGW show that the partial parameters of these shallow groundwater samples exceed standard values (Table 3). The J01 monitoring well was located in the power plant near the bank of the Yangtze River, which is in a low-lying region and in a discharge area of the groundwater flow field. The samples from the J18 well near the west Ash Yard exceeded many standard parameters, which may have been caused by ash infiltration into the shallow groundwater and by slow groundwater movement. The J12 well is located in a livestock farm, and its TH values exceed the standard value. The high TH concentration may be due to human and animal activities, such as using chemical fertilizer and the presence of livestock and domestic sewage.

To further evaluate the shallow groundwater quality in the study area, the rank of each groundwater sample for drinking purposes was calculated using Eq. 3–10, and the results of the groundwater quality assessment in the dry and wet seasons are shown in Table 4. Table 4 reveals that the EWQI values of all the samples range from 19.36 to 61.82 and 23.14–137.33 for the dry and wet seasons, respectively. The critical limit for EWQIs is 100,

**Table 3** Results of the single standard index method for shallow groundwater samples

| Parameters | Dry season | | | Wet season | | |
|---|---|---|---|---|---|---|
| | Max exceed multiple | Exceed ratio (%) | Exceed point | Max exceed multiple | Exceed ratio (%) | Exceed point |
| TH | 3.98 | 18.18 | J12 J18 | 1.7 | 27.27 | J01 J12 J18 |
| pH | 9.02 | 9.09 | J15 | – | – | – |
| TDS | 2.38 | 9.09 | J18 | 1.1 | 9.09 | J01 |
| NO$_2^-$–N | 2.77 | 9.09 | J17 | 1.05 | 9.09 | J07 |
| F$^-$ | 1.54 | 9.09 | J18 | 1.52 | 9.09 | J18 |
| SO$_4^{2-}$ | 5.28 | 18.18 | J01 J18 | 1.74 | 18.18 | J01 J18 |

**Table 4** Results of groundwater quality assessment into dry and wet seasons

| Sample | Dry season | | | wet season | | |
|---|---|---|---|---|---|---|
| | EQWIs | Rank | Water quality | EQWIs | Rank | Water quality |
| J01 | 43.18 | II | Good | 61.82 | III | Medium |
| J03 | 34.25 | II | Good | 36.89 | II | Good |
| J05 | 35.84 | II | Good | 33.21 | II | Good |
| J07 | 26.67 | II | Good | 24.28 | I | Excellent |
| J08 | 33.62 | II | Good | 21.26 | I | Excellent |
| J10 | 23.14 | I | Excellent | 19.36 | I | Excellent |
| J12 | 43.20 | II | Good | 45.31 | II | Good |
| J14 | 26.91 | II | Good | 26.55 | II | Good |
| J15 | 31.24 | II | Good | 23.32 | I | Excellent |
| J17 | 36.92 | II | Good | 29.85 | II | Good |
| J18 | 137.33 | IV | Poor | 55.80 | III | Medium |

indicating that only one sample (J18) in the dry season exceeded the critical limit and is classified as poor-quality water, which suggests that the sample is unsuitable for drinking purposes. In addition, ten groundwater samples are classified as good-quality and excellent-quality water and are, therefore, suitable for human drinking. In addition, nine groundwater samples are categorized as good-quality and excellent-quality water and are fit for human drinking uses, and two groundwater samples (J01 and J18) are categorized as having medium-quality water, and are suited for the centralized production of drinking water sources and for industrial and agricultural water in the wet season. Based on the above results of the single standard index method, TH, TDS, and $SO_4^{2-}$ are the most common contaminants in the study area, which can be confirmed by the hydrochemistry results.

## Groundwater environmental impact assessment

### Numerical simulation of groundwater flow field

To forecast the environmental impacts on groundwater, a numerical model can be used to describe the groundwater flow field (Liu and Wu 2008; Karatzas 2017; Weng et al. 2003; Wu et al. 2015). In this study area, groundwater is mainly recharged by atmospheric precipitation, which is 70% of the total recharge, and the lateral recharged is from the south high-lying region. The groundwater is mainly discharged through soil surface evaporation, through overflow to surface water bodies and through artificial exploitation. Furthermore, the groundwater runoff is approximately from south to north, with a hydraulic gradient ranging from 4 to 6‰, and it is discharged into the Yangtze River. The groundwater depth ranges from 2.3 to 6.9 m, without any obvious changes between each season. According to the above hydrogeological conditions, the simulation area is determined to be approximately 20 km². The edge of the power plant to the banks of the Yangtze River is the boundary of the fixed water level (the first boundary); then, the boundary of fixed flow (the second boundary) is approximately 0.7 km west, 2 km east and 2.8 km south of the power plant, according to the hydrogeological conditions and monitoring sites.

Subsequently, a conceptual hydrogeological model was established for accurately depicting this study area. The simulation area is generalized into one layer, and the hydrogeological parameters are based on those of a phreatic aquifer, where the permeability coefficient is 0.5 m/d, the specific yield is 0.08 and the porosity is 0.6 after recalibration of the model. Based on the given hydrogeological parameters and the equilibrium conditions, we obtain the spatial distribution of the groundwater flow field using this conceptual hydrogeological model. In addition, by fitting the flow field of the same period, we identify the hydrogeological parameters, boundary values, and other equilibrium variables, so that the established model is in accordance with the hydrogeological conditions of the simulation area.

According to the conceptual hydrogeological model and the anisotropy and heterogeneity in water-bearing strata, three-dimensional and unsteady models of groundwater flow consist of a governing equation and of boundary conditions and initial conditions, which are given below, respectively (Liu and Wu 2008; Wu et al. 2017):

$$\begin{cases} \dfrac{\partial}{\partial x}\left(K_{xx}\dfrac{\partial h}{\partial x}\right) + \dfrac{\partial}{\partial y}\left(K_{yy}\dfrac{\partial h}{\partial y}\right) + \dfrac{\partial}{\partial z}\left(K_{zz}\dfrac{\partial h}{\partial z}\right) + W = S\dfrac{\partial h}{\partial t} \\ h(x,y,z) = h_0(x,y,z), (x,y,z) \in \Omega, t = 0 \\ h(x,y,z,t)|_{\Gamma_1} = h(x,y,x,t), (x,y,x,t) \in \Gamma_1, t \geqslant 0 \\ k\dfrac{\partial h}{\partial \vec{n}}\bigg|_{\Gamma_2} = 0 \end{cases}, \tag{11}$$

where $K_{xx}$ is the hydraulic conductivity in the $x$ direction (m/d); $K_{yy}$ is the hydraulic conductivity in the $y$ direction (m/d); $K_{zz}$ is the hydraulic conductivity in the $z$ direction (m/d); S is the specific storage coefficient (1/d); $h$ is the groundwater level (m); $W$ is the source term of groundwater flow (1/d); $h_0(x,y,z)$ is the initial water level; $\Gamma_1$ is the first boundary; and $\Gamma_2$ is the second boundary.

The results of the numerical simulation show that the calculated groundwater flow fields were basically consistent with the measured groundwater flow field in the dry and wet seasons (Fig. 4). As shown in Fig. 4, the dynamic change in the groundwater level at the observed site can accurately reproduce the actual process of groundwater level changes. The corrected model of the numerical simulation basically meets the accuracy requirement, and it can describe the groundwater flow field and match the hydrogeological condition. Overall, this model can be used to forecast groundwater levels and simulate solute transport.

To predict contaminant transport in groundwater, the mathematical model of groundwater solute transport also consists of a governing equation, boundary conditions and initial conditions (Karatzas 2017), which are given by the following equation:

$$R\theta\frac{\partial C}{\partial t} = \frac{\partial}{\partial x_i}\left(\theta D_{ij}\frac{\partial C}{\partial x_{ij}}\right) - \frac{\partial}{\partial x_j}\left(\theta v_i C\right) - \mathrm{WC} \tag{12}$$

where $R$ is the hysteresis coefficient; $\theta$ is the soil porosity; $C$ is the contaminant concentration (mg/L); $D_{ij}$ is the dispersion coefficient (m²/d); $v_i$ is tensor of groundwater velocity; and $W$ is the source term of groundwater flow (1/m).
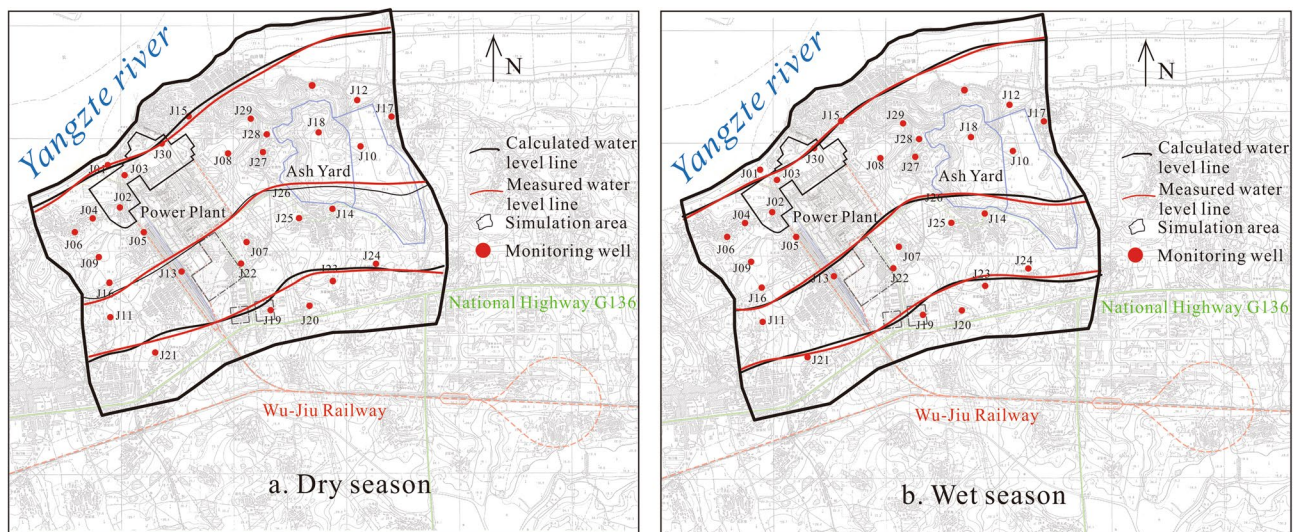
**Fig. 4** Fitting map of the groundwater flow field during the dry and wet seasons

**Table 5** Characteristic pollutants in leakage under abnormal operating conditions

| Circumstance | Particular pollutants | Source intensity (mg/d) | Concentration (mg/L) | Leak pattern |
|---|---|---|---|---|
| Liquid ammonia storage tank leaks | Liquid ammonia | 1388 | 61,700 | Continuous |
| Industrial wastewater treatment sattion leaks | COD | 10,275 | 750 | Continuous |
| | Petroleum | 1644 | 120 | Continuous |
| | Ammonia | 1370 | 100 | Continuous |

## Predicting groundwater environmental impact

According to the power plant design scheme, the leakage of pollutants may have occurred in the semi-underground non-visible areas, such as the liquid ammonia tank, the sewage treatment station, and the industrial wastewater treatment station, which may then seep into the vadose zone and enter shallow groundwater. Of these areas, domestic sewage was sent to the park sewage treatment plant for decontaminating treatment, which not advisable. In this study, the groundwater environmental impacts near the liquid ammonia tank and the industrial wastewater treatment station (Fig. 1) were assessed at the abnormal operating condition leakage point. As shown in Table 5, under the two circumstances of abnormal operating conditions, the pollutants may enter the shallow groundwater. After screening, the four priority control pollutants consist of liquid ammonia, COD, petroleum and ammonia, whose detection limits and analysis methods were recommended by GASQ (III).

Furthermore, groundwater environmental impact assessments conform to the principle of conservative evaluation, which is concerned with the convection–dispersion effect on pollutant transport without regards to the fact that these

pollutants occur from other processes, such as adsorption, volatilization, and biochemistry into the phreatic aquifer of the study area (Karatzas 2017; Zeng et al. 2014). The longitudinal dispersivity and transverse dispersivity of the pollutants were 2.5 and 0.5 m, respectively, calculated by repeatedly adjusting model parameters and empirical values. The concentration distribution of pollutants in the phreatic aquifer can be obtained by solving the equation of groundwater flow (Eq. 11) and pollutant migration (Eq. 12).

The results of the numerical simulation of pollutant migration are shown in Table 6. The results show that the maximum excessive scope of liquid ammonia is 504 m$^2$, which decreases with time during the forecast period and disappears until 40 years of pollutant migration. The maximum migration distance of liquid ammonia increased with time from 26 to 100 m, and the pollution scope first increases and then decreases with a maximum value of 2952 m$^2$. However, excessive values of pollutants are transported approximately 98 m along the groundwater flowlines, and liquid ammonia does not exceed the standard value until the 37th year of pollutant migration in the shallow groundwater (GASQ). Figure 5a shows that the concentration of liquid ammonia changes over time in the monitoring well

**Table 6** Predicted results of pollutant migration

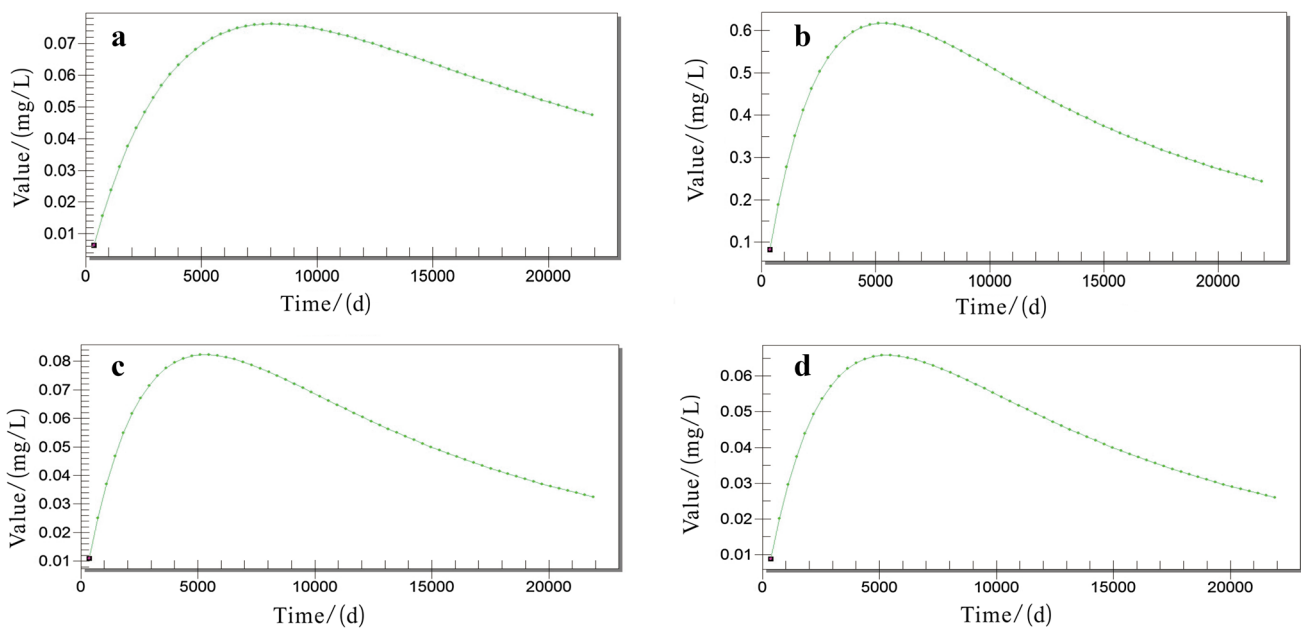| Circumstance | Predictive factor | Pollutant migration time (a) | Pollution scope (m²) | Excessive scope (m²) | Maximum migration distance (m) |
|---|---|---|---|---|---|
| Liquid ammonia storage tank leaks | Liquid ammonia | 1 | 684 | 504 | 26 |
| | | 20 | 2340 | 156 | 62 |
| | | 40 | 2952 | – | 98 |
| | | 60 | 1080 | – | 100 |
| Industrial wastewater treatment sattion leaks | COD | 1 | 1080 | 180 | 26 |
| | | 20 | 1260 | – | 60 |
| | | 40 | 360 | – | 62 |
| | | 60 | – | – | – |
| | Petroleum | 1 | 1120 | 1080 | 24 |
| | | 20 | 2760 | 1245 | 74 |
| | | 40 | 2808 | 375 | 118 |
| | | 60 | 2070 | – | 110 |
| | Ammonia | 1 | 1080 | 540 | 26 |
| | | 20 | 2250 | 183 | 65 |
| | | 40 | 2160 | – | 88 |
| | | 60 | 1080 | – | 110 |



**Fig. 5** Changes in the concentration of pollutants over time in monitoring wells

(J01), and liquid ammonia was detected during the 3rd year of pollutant migration, which finally reached its maximum value of 0.08 mg/L on the 20th year.

For industrial wastewater treatment station leaks, the maximum excessive scope of COD is 180 m², and it disappears until the 20th year of pollutant migration, at which time excessive values of pollutants are transported approximately 26 m along with the groundwater flow. The

concentration of COD was detected on the 6th year of pollutant migration, and it reached a maximum value of 0.68 mg/L on the 13th year in the J03 monitoring well (Fig. 5b). The pollution scope and maximum migration distance disappeared on the 40th year; the maximum pollution scope and maximum migration distance of COD are 1260 and 62 m, respectively. After 40 years, COD does not transport into shallow groundwater (GASQ). Similarly, the

maximum excessive scope of petroleum is 1080 m$^2$ and decreases with time, and it disappeared until 40 years of pollutant migration. After 40 years, the range of excessive values of petroleum transported approximately 118 m along with the groundwater flow, which is also the maximum migration distance. Figure 5c shows that the concentration of petroleum was detected during the second year of pollutant migration and reached the maximum value of 0.075 mg/L on the 14th year in the J03 monitoring well. In the last case, the maximum excessive scope of ammonia is 540 m$^2$, which decreases with time to 375 m$^2$. At this point, the ammonia does not exceed the standard value after 40 years of pollutant migration time, and excessive values of ammonia are transported approximately 88 m along with the groundwater flow, but the maximum migration distance continuously increases to 110 m. However, the pollution scope increases first and then decreases from 1080 to 2250 m$^2$, and becomes progressively smaller, returning to the initial value of 1080 m$^2$ after 60 years of pollutant migration time. From the date of monitoring well (J03), ammonia was detected in the first year of pollutant migration time and reached the maximum value of 0.08 mg/L in the 14th year, which decreases annually until it disappears (Fig. 5d).

## Conclusions

In the study area, the shallow groundwater in the dry and wet seasons contains major ions in the relative concentrations of $Ca^{2+} > Na^+ > Mg^{2+} > K^+$ for cations and $HCO_3^- > SO_4^{2-} > Cl^-$ for anions. The statistical results of other ions suggest that the groundwater has been polluted by human activities in the past and either the source of pollution has been removed or that groundwater quality is improving due to biochemical reactions in the aquifer. The results show that the shallow groundwater has slightly high hardness and alkalinity. In general, the hydrochemical facies are predominantly of the $HCO_3$–Ca type, and rock weathering is likely to be the most important process controlling groundwater chemistry at this study site. In addition, we characterize the groundwater quality for drinking purposes based on the shallow groundwater quality indices using the single standard index method and the entropy-weighted water quality index at the power plant. The results reveal that 81.81% of the groundwater samples are categorized as good quality and excellent quality, and most of the shallow groundwater from the dry and wet seasons is of suitable quality for potable use, except for three sites (J01, J12 and J18) that were polluted by human activities.

Based on this detailed information about shallow groundwater chemistry and the groundwater quality assessment, an established model of numerical simulation is used for evaluating the groundwater environmental impact from the power plant operation. The results show that the pollutants of abnormal operating condition leakage consist of liquid ammonia, COD, petroleum and ammonia, and they do not exceed the standard value until they disappear after many years of migration time. The pollutants also do not exceed the boundary of the simulated area to enter into the Yangtze River. Overall, these risks of contamination are acceptable according to the most conservative principles of environmental protection. Therefore, it is necessary to carry out effective anti-seepage measures for key areas in the power plant and to put forward emergency measures and pollution control measures.

## References

Ahada CPS, Suthar S (2017) Hydrochemistry of groundwater in North Rajasthan, India: chemical and multivariate analysis. Environ Earth Sci 76(5):203

Amiri V, Rezaei M, Sohrabi N (2014) Groundwater quality assessment using entropy weighted water quality index (EWQI) in Lenjanat, Iran. Environ Earth Sci 72(9):3479–3490

Bureau of Quality and Technical Supervison of China (1994) National Standard of the People's Republic of China: Quality Standard for Groundwater, GB/T 14848-93 (in Chinese)

Chanchal, Hussain A (2015) Groundwater quality assessment around ash pond of Parichha thermal power plant, Jhansi, India. Asian J Water Environ Pollut 12(3):83–88

Garcia MG, Hidalgo MD, Blesa MA (2001) Geochemistry of groundwater in the alluvial plain of Tucuman province, Argentina. Hydrogeol J 9(6):597–610

Gibbs RJ (1970) Mechanisms controlling world water chemistry. Science 170:1088–1090

Gohari A, Eslamian S, Mirchi A, Abedi-Koupaei J, Bavani AM, Madani K (2013) Water transfer as a solution to water shortage: a fix that can backfire. J Hydrol 491(1):23–39

Güler C, Kurt MA, Alpaslan M, Akbulut C (2012) Assessment of the impact of anthropogenic activities on the groundwater hydrology and chemistry in Tarsus coastal plain (Mersin, SE Turkey) using fuzzy clustering, multivariate statistics and GIS techniques. J Hydrol 414(3):435–451

Hayat E, Baba A (2017) Quality of groundwater resources in Afghanistan. Environ Monit Assess 189(7):318

He BY, Xu GL (2000) The problems in use of water resource of Hubei Province and its strategic countermeasures. Resour Environ Yangtze Basin 9:207–211 (in Chinese)

Islam ARMT, Ahmed N, Bodrud-Doza M, Chu RH (2017) Characterizing groundwater quality ranks for drinking purposes in Sylhet district, Bangladesh, using entropy method, spatial autocorrelation index, and geostatistics. Environ Sci Pollut Res 24(34):26350–26374

Kamrani S, Rezaei M, Amiri V, Saberinasr A (2016) Investigating the efficiency of information entropy and fuzzy theories to classification of groundwater samples for drinking purposes: Lenjanat Plain, Central Iran. Environ Earth Sci 75(20):1370

Karatzas GP (2017) Developments on modeling of groundwater flow and contaminant transport. Water Resour Manage 31(10):3235–3244

Kim GB (2015) Optimal distribution of groundwater monitoring wells near the river barrages of the 4MRRP using a numerical model and topographic analysis. Environ Earth Sci 73(9):5497–5511

Lap BQ, Mori K, Inoue E (2007) A one-dimensional model for water quality simulation in medium- and small-sized rivers. Paddy Water Environ 5(1):5–13

Li PY, Wu JH, Qian H (2010) Groundwater quality assessment based on entropy weighted osculating value method. Int J Environ Sci 27(3):31–34

Li PY, Wu JH, Qian H (2013) Assessment of groundwater quality for irrigation purpose and identification of hydrogeochemical evolution mechanisms in Pengyang County, China. Environ Earth Sci 69(7):2211–2225

Li PY, Qian H, Wu JH, Chen J, Zhang Y, Zhang H (2014) Occurrence and hydrogeochemistry of fluoride in alluvial aquifer of Weihe River, China. Environ Earth Sci 71(7):3133–3145

Li PY, Wu JH, Qian H, Zhang Y, Yang N, Jing L (2016a) Hydrogeochemical characterization of groundwater in and around a wastewater irrigated forest in the Southeastern Edge of the Tengger Desert, Northwest China. Exposure Health 8(3):331–348

Li J, Yang Y, Huan H, Li M, Xi B, Lv N (2016b) Method for screening prevention and control measures and technologies based on groundwater pollution intensity assessment. Sci Total Environ 551–552:143–154

Li Z, Li CH, Wang X, Peng C, Cai Y, Huang W (2018) A hybrid system dynamics and optimization approach for supporting sustainable water resources planning in Zhengzhou City, China. J Hydrol 556:50–60

Liu Y, Wu XF (2008) Numerical methods comparison in simulating contaminants movement in groundwater. Chin J Environ Eng 2:229–234 (in Chinese)

Marghada D, Malpe DB, Zade AB (2012) Major ion chemistry of shallow groundwater of a fast growing city of Central India. Environ Monit Asses 184(4):2405–2418

Murkute YA (2014) Hydrogeochemical characterization and quality assessment of groundwater around Umrer coal mine area Nagpur District, Maharashtra, India. Environ Earth Sci 72(10):4059–4073

Peng C, He JT, Wang ML, Zhang ZG, Wang L (2017) Identifying and assessing human activity impacts on groundwater quality through hydrogeochemical anomalies and $NO_3^-$, $NH_4^+$, and COD contamination: a case study of the liujiang river basin, Hebei province, P.R. China. Environ Sci Pollut Res 2:1–18

Qian C, Wu X, Mu WP, Fu RZ, Zhu G, Wang ZR, Wang DD (2016) Hydrogeochemical characterization and suitability assessment of groundwater in an agro-psatoral area, Ordos Basin, NW China. Environ Earth Sci 75(20):1356

Shao DG, Wang ZM, Wang B, Luo WW (2016) A water quality model with three dimensional variational data assimilation for contaminant transport. Water Resour Manage 30(13):4501–4512

Su H, Kang WD, Xu YJ, Wang JD (2017) Assessment of groundwater quality and health risk in the oil and gas field of Dingbian County, Northwest China. Expo Health 9(4):227–242

Vandenbohede A, Hinsby K, Courtens C, Lebbe L (2011) Flow and transport model of a polder area in the Belgian coastal plain: example of data integration. Hydrogeol J 19(8):1599–1615

Varnosfaderany MN, Mirghaffary N, Ebrahimi E, Soffianian A (2009) Water quality assessment in an arid region using a water quality index. Water Sci Technol 60(9):2319–2327

Venkataraman K, Tummuri S, Medina A, Perry J (2016) 21st century drought outlook for major climate divisions of texas based on cmip5 multimodel ensemble: implications for water resource management. J Hydrol 534:300–316

Weng BH, Chen GL, Xiang QG (2003) Evaluation method for influence of gas-field water on shallow groundwater. Nat Gas Ind 23:153–156 (in Chinese)

Winton RS, Moorman M, Richardson CJ (2016) Waterfowl impoundments as sources of nitrogen pollution. Water Air Soil Pollut 227(10):390

Wu Z, Fu XD, Wang GQ (2015) Concentration distribution of contaminant transport in wetland flows. J Hydro 525:335–344

Wu C, Wu X, Qian C (2017) Pollutants of gas field development effect on groundwater environment in Hangjin Banner. J China Coal Society 12:3262–3269 (in Chinese)

Xiao J, Jin ZD, Wang J (2014) Assessment of the hydrogeochemical and groundwater quality of the Tarim River Basin in an extreme arid region, NW China. Environ Manage 53(1):135–146

Yan BW, Chen L (2013) Coincidence probability of precipitation for the middle route of south-to-north water transfer project in China. J Hydro 499(9):19–26

Zeng L, Zhao YJ, Chen B, Ji P, Wu YH, Feng L (2014) Longitudinal spread of bicomponent contaminant in wetland flow dominated by bank-wall effect. J Hydro 509(4):179–509

Zhang XY, Xin BD, Liu WC, Guo GX, Lu HY, Ji ZQ (2011) Comparative analysis on three evaluation methods for groundwater quality assessment. J Water Resour Water Eng 22:113–118 (in Chinese)

Zhang XH, Wu YY, Gu BJ (2015) Urban rivers as hotspots of regional nitrogen pollution. Environ Pollut 205:139–144